ELSEVIER

HIV-1 Infection Kinetics in Tissue Cultures

JOHN L. SPOUGE*
National Center for Biotechnology Information, National Library of Medicine, Bethesda, Maryland USA

RICHARD I. SHRAGER
Physical Sciences Laboratory, DCRT, National Institute of Health, Bethesda, Maryland USA

AND

DIMITER S. DIMITROV
Laboratory of Mathematical Biology, NCI, National Institutes of Health, Bethesda, Maryland USA

Received 13 November 1995; revised 26 March 1996

ABSTRACT

Despite intensive experimental work on HIV-1, very little theoretical work has focused on HIV-1 spread in tissue culture. This article uses two systems of ordinary differential equations to model two modes of viral spread, cell-free virus and cell-to-cell contact. The two models produce remarkably similar qualitative results. Simulations using realistic parameter regimes showed that starting with a small fraction of cells infected, both cell-free viral spread and direct cell-to-cell transmission give an initial exponential phase of viral growth, followed by either a crash or a gradual decline, extinguishing the culture. Under some conditions, an oscillatory phase may precede the extinction. Some previous models of in vivo HIV-1 infection oscillate, but only in unrealistic parameter regimes. Experimental tissue infections sometimes display several sequential cycles of oscillation, however, so our models can at least mimic them qualitatively. Significantly, the models show that infective oscillations can be explained by infection dynamics; biological heterogeneity is not required. The models also display proportionality between infected cells and cell-free virus, which is reassuringly consistent with assumptions about the equivalence of several measures of viral load, except that the proportionality requires a relatively constant total cell concentration. Tissue culture parameter values can be determined from accurate, controlled experiments. Therefore, if verified, our models should make interpreting experimental data and extrapolating it to in vivo conditions sharper and more reliable.

*To whom correspondence should be addressed.

MATHEMATICAL BIOSCIENCES 138:1–22 (1996)

655 Avenue of the Americas, New York, NY 10010
0025-5564/96/$15.00
PII S0025-5564(96)00064-8

1. INTRODUCTION

About half a century ago, Delbrueck among others used experimental techniques and theoretical modeling to study bacteriophages [1, 2]. Some fundamental genetic concepts followed from his experiments, which had to be designed to answer precisely posed theoretical questions. In an extension of the bacteriophage studies to animal virology, Dulbecco and co-workers introduced his plaque assay and complemented it with mathematical modeling [3, 4]. Concepts derived from these studies, e.g., multiplicity of infection (MOI) [5], are now used routinely when characterizing virtually any animal virus.

Many mathematical models examine the in vivo effects of human immunodeficiency virus type 1 (HIV-1) infection and its interactions with the immune system (see, e.g., [6]). As with many animal viruses, however, most of our knowledge about the replication of HIV-1 derives from in vivo infection of tissue cultures. In light of the intensive experimental work, surprisingly little theoretical work has focused on HIV-1 spread in tissue culture, particularly when compared to the theoretical bacteriophage studies of the late 1930s. Of the theories examining HIV-1 infection in tissue culture (e.g., [7]), two are particularly relevant to this paper.

The first theory explored the infection kinetics of cell-free HIV-1 by viewing the viral lifetime as a race between HIV attachment and inactivation [8]. This view eventually crystallized in the concept of viral multiplicity of attachment (MOA). A virion's MOA in a particular time interval is the average number of cellular attachment opportunities that must be blocked to keep the virion in suspension [9]. The number of attachment opportunities, the virion's MOA, is usually proportional to both virus-cell incubation time and cell concentration. During a typical in vitro incubation of 1 h in 5×10^5 cells/ml, a virion from a laboratory HIV-1 strain has an MOA of around 1; i.e., it has about one attachment opportunity. (The corresponding MOA for a virion from a primary isolate is probably somewhat higher [10].) The MOA concept quantifies observations that blocking viral attachment in culture [11] and clinically [8, 12–14] is more difficult as cell concentrations or incubation times increase. This theory is used to estimate the number of attachment opportunities for a virion, to show that under culture conditions individual virions generally attach before they inactivate.

The second theory quantified the exponential spread of HIV-1 during cycles of infection in tissue culture [15]. The semi-empirical formulas from the theory determined two significant parameters of HIV-1 infection, the number of infecting virions produced by one cell in one cycle of infection and the time required to complete one cycle of infection. Although this theory has applications to quantifying both the

infectivity of HIV-1 and the efficacy of HIV-1 inhibitors, its validity has been limited to the initial phases of viral spread because it neglects cell death and other progressive restrictions on viral expansion. In addition, it does not directly examine factors changing free virus attachment, the relative importance of cell-to-cell contact, cell-free virus to viral spread, etc. This theory is used here to estimate parameters from data on initial viral spread.

Here, we present a model of HIV-1 infection kinetics in tissue cultures. The model is based on a system of differential equations, similar to models of HIV-1 infection kinetics in vivo (e.g., [6]). Unlike the previous models, however, our model explicitly takes into account whether viral spread takes place through cell-to-cell contacts or suspension virions, because the distinction may be important [15–17]. Tissue culture infection is inherently simpler than infection in vivo, and parameter values can be determined from accurate, controlled experiments. Therefore, if verified, our model may make interpreting experimental data and extrapolating it to in vivo conditions sharper and more reliable.

2. MODEL

Table 1 lists the symbols in this paper. The parameter values are justified, when required, from the references given or else derived in Section 5.

2.1. *CELL GROWTH IN THE ABSENCE OF INFECTION*

This article models changes in cell concentration in the absence of infection and without external cell sources as [6]

$$\begin{aligned}\frac{dC}{dT} &= rC\left[1-(C+\gamma M)C_{\max}^{-1}\right]-\mu_C C \\ &= r_C C\left[1-(C+\gamma M)C_m^{-1}\right] \qquad (1)\\ \frac{dM}{dT} &= \mu_C C.\end{aligned}$$

The first form of dC/dT uses direct physical constants, but the second, simpler form is used in later extensions of Eq. (1).

The first term in Eq. (1) quantifies the reproduction of the cells and contains a phenomenological factor that prevents healthy cells from reproducing when the system reaches its carrying capacity $C_{\max}$ [18, p. 71]. Equation (1) allows that a dead cell might slow the reproduction of healthy cells through metabolic poisons, etc., although perhaps less than a healthy cell (thus $0 \leqslant \gamma \leqslant 1$).

The dead cells may degrade into cellular debris. Degradation can be handled by adding corresponding terms and equations, but we prefer a

TABLE 1

Parameter Ranges and Default or Initial Values

DEPENDENT VARIABLES	
C concentration of healthy cells	[5×10^5 ml^{-1}]
I concentration of infected cells	[5×10^2 ml^{-1}]
M concentration of cells that have died	[0 ml^{-1}]
S continuous splitting volume	
T time	
V concentration of physical cell-free viral particles	[5×10^5 ml^{-1}]
PARAMETERS AND CONSTANTS	
C_{max} carrying capacity of healthy cells	[(2–5) 2×10^6 ml^{-1} [12]]
k_e empirical initial growth rate of virus	[(0.3–1.5) 1 day^{-1} [15]]
k_A attachment rate constant for infectious virions	[(2–6) 2×10^{-5} ml^{-1} day^{-1} [9]]
k_I rate constant for cell-to-cell spread	[(1–3) 2×10^{-6} ml^{-1} day^{-1} (Section 5)]
k_S hypothetical rate constant for continuous splitting	[(0.0–0.7) 0.7 day^{-1} (Section 4.3)]
r healthy cell reproductive rate constant	[(0.0–0.7) 0.7 day^{-1} [15]]
r_P rate constant at which infected cells produce virions	[(10^2–10^5) 2×10^3 day^{-1} [15]]
γ relative reduction in the carrying capacity due to dead cells and cellular debris	[(0–1) 0]
ϵ relative efficiency of viral attachment to dead vs. live cells	[(0–1) 0]
μ_C rate constant at which healthy cells die	[0.02 day^{-1} [6]]
μ_I rate constant at which infected cells die	[(0.2–1) 0.3 day^{-1} [29]]
μ_V nonspecific inactivation rate constant for virions	[(0.3–2) 1 day^{-1} [26]]
σ ratio of physical particles attaching to infections	[(10^{-4}–10^{-7}) 5×10^{-4}] [15, 26]
DERIVED QUANTITIES	
$C_m = r^{-1}(r-\mu_C)C_{max}$ effective carrying capacity of healthy cells	[2×10^6 ml^{-1}]
c^* reduced concentration of healthy cells from Eq. (8)	
i^* reduced concentration of infected cells from Eq. (8)	
$r_C = r-\mu_C$ effective healthy cell reproductive rate constant	[0.68 day^{-1}]
$r_S = r_P\sigma$ rate constant for infected cells producing infecting virions	[1 day^{-1}]
$\rho_C = r-(1-\epsilon)\mu_C = r_C+\epsilon\mu_C$	[0.68 day^{-1}]

simpler, more phenomenological approach that includes the effect of dead cells and cellular debris in a single quantity M.

2.2. *SPREADING INFECTION BY CELL-TO-CELL CONTACT*

In a typical tissue culture, cell-to-cell spread is often thought to be the dominant mode of viral transmission [15–17]. This article models cell-to-cell spread as a Lotka–Volterra predator–prey system [19], with the healthy cells as the prey and the infected cells as the predators. To determine whether cell-to-cell spread has kinetic features distinguishing it from spread by cell-free virions, we consider the two types of viral

transmission separately, although the corresponding equations, Eqs. (2) and (3), could have been combined in an obvious (but unwieldy) way.

Accordingly, Eq. (2) models the spread of infection by cell-to-cell contact and ignores spread by cell-free virions:

$$\begin{aligned} \frac{dC}{dT} &= -k_I IC + r_C C\left[1-(C+I+\gamma M)C_m^{-1}\right] \\ \frac{dI}{dT} &= k_I IC - \mu_I I \\ \frac{dM}{dT} &= \mu_C C + \mu_I I. \end{aligned} \tag{2}$$

Like Eq. (1), Eq. (2) allows that dead cells and cellular debris can slow healthy cell reproduction, but it also assumes that the carrying capacity and any signals controlling the reproduction of healthy cells (e.g., metabolic wastes, cytokines) can be influenced by both the total number of live cells (without regard to cell status as healthy or infected) and the total number of cells that have died.

The terms $k_I IC$, representing cell-to-cell spread, are appropriate in a system if the cells are well mixed [8], an assumption deserving some scrutiny. Although isolated lymphocytes are mobile, tissue culture systems are generally not well mixed, and a cell usually maintains its contact with neighbors. Occasionally, however (usually every second or third day), tissue culture cells may be split, with some cells being removed and the culture diluted, thereby mixing the system. This partially justifies using the terms $k_I IC$ in Eq. (2).

Equation (2) does not include a latent period after cells have been infected. Latency might be modeled either by a delay, e.g., $I(t-\tau)$ instead of $I(t)$, or by an explicit class of latently infected cells $L(t)$ [6]. For simplicity, we have omitted latency because it is fast (about a day [20]) on the time scales of interest here (at least a week).

Proving that all concentrations remain nonnegative under Eqs. (2) [and (3) below] is straightforward and is omitted.

2.3. *SPREADING INFECTION BY CELL-FREE VIRIONS*

This section distinguishes carefully between infectious and physical viral particles. Measuring infectivity gives the number of infecting viral particles in a viral stock; electron microscopy estimates the number of physical viral particles.

As a complement to Eq. (2), Eq. (3) models the spread of infection by cell-free virions and ignores spread by cell-to-cell contact:

$$\begin{aligned}
\frac{dC}{dT} &= -k_A \sigma VC + r_C C\left[1-(C+I+\gamma M)C_m^{-1}\right] \\
\frac{dI}{dT} &= k_A \sigma VC - \mu_I I \\
\frac{dM}{dT} &= \mu_C C + \mu_I I \\
\frac{dV}{dT} &= r_P I - k_A V(C+I+\epsilon M) - \mu_V V.
\end{aligned} \tag{3}$$

The terms $k_A \sigma VC$ representing infection by a cell-free virion resemble the terms $k_I IC$ in Eq. (2), except that only a successful fraction σ of the physical cell-free virions attaching to a cell infect it. Table 1 approximates σ by the ratio of infectious to physical viral particles in an HIV stock. Computer simulations based on this approximation are not at variance with experimental data (see the Discussion). The reproductive parameter r_P in Table 1 also refers to physical particles, and while Eq. (2) does not explicitly link viral production $r_P I$ to infected cell death, the ratio $r_P \mu_I^{-1}$ could be interpreted as the average number of physical particles released by a lysing infected cell [6].

Like Eq. (2), Eq. (3) assumes a well-mixed system. In this case, the system must maintain mixing of suspension virions and cells. This assumption appears justified in many but not all experimental systems [21–25]. For the same reason as for Eq. (2), Eq. (3) also does not include a latent period after cells have been infected.

The parameter $0 \leqslant \epsilon \leqslant 1$ is a relative attachment efficiency, the ratio of viral attachment rates to dead cells and live cells. As with its carrying capacity terms, Eq. (2) permits its viral attachment terms to distinguish live cells from dead cells, but is indifferent to the cells' status as healthy or infected. Note that even if dead cells eventually disintegrate, they still may decoy some virions from attaching to live cells. Decoying virus with dead cells and cellular debris is a novel feature in our model and has some interesting consequences.

3. ANALYSIS

3.1. *SPREADING INFECTION BY CELL-TO-CELL CONTACT*

3.1.1. *Short-Time Exponential Growth*

When substituted into Eq. (2), the initial values of (C, I, M) give the exponential growth of healthy cells at time $T = 0$ as $C^{-1}(dC/dT) =$

$-k_I I + r_C[1-(C+I+\gamma M)C_m^{-1}]$; and the corresponding empirical exponential growth rate k_e for infected cells, as $k_e = I^{-1}(dI/dT) = k_I C - \mu_I$.

For cell-to-cell spread, the initial exponential growth of infected cells is a linear function of the initial concentration of infected cells.

3.1.2. Medium-Time Evolution ($\gamma MC_m^{-1} \ll 1-(C+I)C_m^{-1}$)

For $\gamma MC_m^{-1} \ll 1-(C+I)C_m^{-1}$, Eqs. (2) have equilibrium points

$$\begin{aligned} \frac{dC}{dt} = 0 \quad &\Rightarrow \quad C = 0 \quad \text{or} \quad -k_I I + r_C\left[1-(C+I)C_m^{-1}\right] = 0 \\ \frac{dI}{dt} = 0 \quad &\Rightarrow \quad I = 0 \quad \text{or} \quad k_I C - \mu_I = 0 \end{aligned} \tag{4}$$

and Jacobian

$$\mathbf{J} = \begin{pmatrix} -k_I I + r_C\left[1-(C+I)C_m^{-1}\right] - r_C C C_m^{-1} & -C\left(k_I + r_C C_m^{-1}\right) \\ k_I I & k_I C - \mu_I \end{pmatrix}. \tag{5}$$

One combination from Eqs. (4), $C = 0$ and $k_I C - \mu_I = 0$, is clearly contradictory, since $\mu_I > 0$ (infected cells die). The three equilibrium points remaining and their eigenvalues λ, which solve $\det(\mathbf{J} - \lambda\mathbf{I}) = 0$, are $(0,0)$ with eigenvalues $\lambda = r_C$ and $\lambda = -\mu_I$; $(C_m, 0)$ with eigenvalues $\lambda = -r_C$ and $\lambda = k_I C_m - \mu_I$; and $(C_i, I_i) = (\mu_I k_I^{-1}, r_C(1-\mu_I k_I^{-1} C_m^{-1})(k_I + r_C C_m^{-1})^{-1})$ with eigenvalues satisfying

$$\lambda^2 + r_C \mu_I k_I^{-1} C_m^{-1}\lambda + r_C \mu_I\left(1-\mu_I k_I^{-1} C_m^{-1}\right) = 0. \tag{6}$$

All eigenvalues from Eq. (6) have a negative real part (although both signs for the discriminant of Eq. (6) can occur). The third point (C_i, I_i) satisfies $I_i > 0$ only when $k_I C_m > \mu_I$.

Thus there are two principal cases, separated by the borderline case $k_I C_m = \mu_I$.

Case 1: Healthy cells predominate and infected cells die exponentially. If $k_I C_m < \mu_I$, $(0,0)$ is a saddle point, while $(C_m, 0)$ is an asymptotically stable star (our stability terminology follows [18]). In this case, the third point (C_i, I_i) is unphysical.

The equilibrium values $(C_m, 0)$ when substituted into Eq. (2) give the asymptotic exponential growth of healthy cells as $C_{eq}^{-1}(dC/dT)_{eq} = 0$ and of infected cells, as $I_{eq}^{-1}(dI/dT)_{eq} = k_I C_m - \mu_I < 0$.

Case 2: Healthy cells and infected cells coexist. If $k_I C_m > \mu_I$, $(0,0)$ is still a saddle point, but $(C_m, 0)$ has also become a saddle point. (C_i, I_i) has become physical and is an asymptotically stable star if the discriminant of Eq. (6) is positive or an asymptotically stable spiral if it is negative.

The equilibrium values (C_i, I_i) when substituted into Eq. (2) give zero asymptotic growth: $C_{eq}^{-1}(dC/dT)_{eq} = I_{eq}^{-1}(dI/dT)_{eq} = 0$. The approach to zero growth is steady if the discriminant of Eq. (6) is positive, but gives damped oscillations if it is negative.

3.1.3. *Long-Time Death*

Assume $\gamma > 0$. If C or I were bounded away from 0 for an infinite total time, the equation for dM/dT in Eq. (2) shows that M eventually would exceed any preassigned bound, e.g., $2\gamma^{-1}C_m$. $M \geqslant 2\gamma^{-1}C_m$ implies that $d(C+I)/dT \leqslant -[\min(r_C, \mu_I)](C+I)$, however, driving both C and I to 0 exponentially fast. Thus, ultimately the dead cells and cellular debris choke and kill the system.

3.2. *SPREADING INFECTION BY CELL-FREE VIRIONS*

3.2.1. *Quasi-Steady-State Approximation*

Viral processes in the suspension phase are usually faster than cellular processes. This observation justifies a quasi-steady-state approximation $dV/dT \approx 0$ in analyzing Eq. (3):

$$V \approx \frac{r_P I}{k_A(C + I + \epsilon M) + \mu_V}. \tag{7}$$

A similar quasi-steady-state approximation was accurate in an in vivo model [6]; numerical runs also confirmed the accuracy here.

Substituting Eq. (7) into Eqs. (3) suggests the use of "reduced variables":

$$\begin{aligned} c^* &= \frac{k_A C}{k_A(C + I + \epsilon M) + \mu_V} \\ i^* &= \frac{k_A I}{k_A(C + I + \epsilon M) + \mu_V}. \end{aligned} \tag{8}$$

3.2.2. *Short-Time Exponential Growth*

After the viral quasi-steady state in Eq. (7) has been established, the reduced variables and Eqs. (3) give

$$\begin{aligned} \frac{d\ln C}{dT} &= -r_S i^* + r_C\left[1-(C+I+\gamma M)C_m^{-1}\right] \\ \frac{d\ln I}{dT} &= r_S c^* - \mu_I . \end{aligned} \tag{9}$$

The initial values of (c^*, i^*) after viral quasi-steady state has been established, when substituted into Eq. (9), give the short-time exponential growth of healthy cells as $-r_S i^* + r_C[1-(C+I+\gamma M)C_m^{-1}]$ and the corresponding exponential growth rate k_e for infected cells as $k_e = r_S c^* - \mu_I$. Thus, if $(C+I+\gamma M)C_m^{-1} \ll 1$ so the system is well below its effective carrying capacity, the initial exponential rate of infection depends only on c^* and i^*. If in addition $\mu_V \ll k_A(C+I+\epsilon M)$ so virions have several attachment opportunities before inactivating [9], and if $\epsilon M \ll C+I$, so they preferentially attach to live cells, c^* and i^* depend only on the proportion of infected cells $I(C+I)^{-1}$. For spread by cell-free virions (under these assumptions), the initial exponential growth of infected cells and virus depends on the initial (quasi-equilibrated) proportion of infected cells and not on their concentration.

3.2.3. *Medium-Time Evolution* $((C+I+\gamma M)C_m^{-1} \ll 1)$

While the assumption $\gamma M C_m^{-1} \ll 1-(C+I)C_m^{-1}$ is symmetric with the previous section, and thus aesthetically desirable, it does not simplify the mathematics.

In Eq. (9), if $(C+I+\gamma M)C_m^{-1} \ll 1$ so the system is initially below its effective carrying capacity, the medium-time behavior depends only on the reduced variables. This observation motivates examining the asymptotic phase plane behavior of c^* and i^*.

For $(C+I+\gamma M)C_m^{-1} \ll 1$, Eq. (8) puts Eq. (3) into the form:

$$\begin{aligned} \frac{dc^*}{dT} &= c^*\left\{-\rho_C c^* + \left[(1-\epsilon)\mu_I - r_S\right]i^* + r_C\right\} \\ \frac{di^*}{dT} &= i^*\left[(r_S-\rho_C)c^* + (1-\epsilon)\mu_I i^* - \mu_I\right]. \end{aligned} \tag{10}$$

Equations (10) preserve $0 \leqslant c^*$ and $0 \leqslant i^*$. By manipulating Eqs. (10), the three inequalities $0 \leqslant c^*$, $0 \leqslant i^*$, and $c^* + i^* \leqslant 1$ imply that $d\ln[1-(c^*+i^*)]/dT \geqslant -r_C$, so they are preserved over time, which is also obvious from Eq. (8) and physical intuition.

Equations (10) have equilibrium points

$$\begin{aligned} \frac{dc^*}{dt} = 0 \quad &\Rightarrow \quad c^* = 0 \quad \text{or} \quad -\rho_C c^* + [(1-\epsilon)\mu_I - r_S] i^* + r_C = 0 \\ \frac{di^*}{dt} = 0 \quad &\Rightarrow \quad i^* = 0 \quad \text{or} \quad (r_S - \rho_C) c^* + (1-\epsilon)\mu_I i^* - \mu_I = 0 \end{aligned} \tag{11}$$

and Jacobian

$$J = \begin{pmatrix} -2\rho_C c^* + [(1-\epsilon)\mu_I - r_S] i^* + r_C & [(1-\epsilon)\mu_I - r_S] c^* \\ (r_S - \rho_C) i^* & (r_S - \rho_C) c^* + 2(1-\epsilon)\mu_I i^* - \mu_I \end{pmatrix}. \tag{12}$$

One combination from Eqs. (11) produces $(c_\epsilon^*, i_\epsilon^*) = (0, (1-\epsilon)^{-1})$. The point $(c_\epsilon^*, i_\epsilon^*)$ is physical only for $\epsilon = 0$ when it equals $(0,1)$. Even then, it has eigenvalues $\lambda = -(r_S - \mu_I - r_C)$ and $\lambda = \mu_I$, is not stable, and need not be considered further. The three points remaining and their eigenvalues λ are $(0,0)$ with eigenvalues $\lambda = r_C$ and $\lambda = -\mu_I$; $(r_C \rho_C^{-1}, 0)$ with eigenvalues $\lambda = -r_C$ and $\lambda = r_C \rho_C^{-1} r_S - r_C - \mu_I$; and

$$(c_v^*, i_v^*) = \left(\frac{\mu_I [r_S - (1-\epsilon)(r_C + \mu_I)]}{r_S [r_S - \rho_C - (1-\epsilon)\mu_I]}, \frac{\rho_C (r_C \rho_C^{-1} r_S - r_C - \mu_I)}{r_S [r_S - \rho_C - (1-\epsilon)\mu_I]} \right) \tag{13}$$

with eigenvalues satisfying

$$\lambda^2 + [\rho_C c_v^* - (1-\epsilon)\mu_I i_v^*] \lambda + r_S [r_S - \rho_C - (1-\epsilon)\mu_I] c_v^* i_v^* = 0. \tag{14}$$

The eigenvalues have a nonpositive real part since the coefficient of λ is

$$\begin{aligned} \rho_C c_v^* - (1-\epsilon)\mu_I i_v^* &= -r_S i_v^* + r_C \\ &= r_S c_v^* - \mu_I = \epsilon \frac{\mu_I (r_C + \mu_C)}{r_S - \rho_C - (1-\epsilon)\mu_I}. \end{aligned} \tag{15}$$

Both signs for the discriminant of Eq. (14) can occur. By algebra, $0 \leqslant c_v^*$, $0 \leqslant i_v^*$ and $c_v^* + i_v^* \leqslant 1$ only if all the numerators and denominators in c_v^* and i_v^* are nonnegative. This implies that $0 \leqslant r_C \rho_C^{-1} r_S - r_C - \mu_I$ and that the common value in Eq. (15) is nonnegative.

There are two principal cases, separated by the borderline case $r_C \rho_C^{-1} r_S = r_C + \mu_I$.

Case 1: Healthy cells predominate and infected cells die exponentially. If $r_C \rho_C^{-1} r_S < r_C + \mu_I$, (0,0) is a saddle point, while $(r_C \rho_C^{-1}, 0)$ is an asymptotically stable star. In this case, the third point (c_v^*, i_v^*) is unphysical.

Equations (9) show that in this case, the medium-time exponential growth of healthy cells is $r_C > 0$, and the medium-time exponential growth of infected cells is $-(\mu_I - r_C \rho_C^{-1} r_S) < 0$.

Case 2: Healthy cells and infected cells coexist. If $r_C \rho_C^{-1} r_S > r_C + \mu_I$, (0,0) is still a saddle point, but $(r_C \rho_C^{-1}, 0)$ has also become a saddle point. The point (c_v^*, i_v^*) has become physical. If the discriminant of Eq. (14) is positive, (c_v^*, i_v^*) is an asymptotically stable star; otherwise, it is a spiral if $\epsilon > 0$, or a center if $\epsilon = 0$.

Equations (9) show that in this case, the medium-time exponential growth of both healthy and infected cells is $-r_S i_v^* + r_C = r_C c_v^* - \mu_I \geqslant 0$. The ratio of infected to healthy cells approaches i_v^* / c_v^*. The approach to these values is steady if the discriminant of Eq. (14) is positive; if, however, the discriminant is negative, $\epsilon > 0$ gives damped oscillations. All else equal, these oscillations become less damped as ϵ decreases (cf. Eqs. (14) and (15)), until they are undamped at $\epsilon = 0$. In other words, the oscillations become less prominent the more that dead cells and cellular debris decoy cell-free virions.

3.2.4. *Long-Time Death*

As with cell-to-cell spread (and with a similar proof), ultimately the dead cells and cellular debris choke and kill the system.

3.3. *SPLITTING A CULTURE AND ITS EFFECT*

Sometimes tissue culture cells are split, with some cells being removed and the culture diluted. If done, splitting usually divides the culture in half every second or third day, with medium being added to expand the volume of the two halves to match the original volume.

Although numerical simulations is required to assess the quantitative effects of splitting, the following mathematical approximation of "continuous splitting" correctly anticipates many of the qualitative effects. Even though splitting is discrete, approximate it by a steady, exponential increase in the culture volume, and let the equation describing the splitting volume be $S = S(0)e^{k_S t}$. The volume increase is then equivalent to adding the terms $-k_S C$, $-k_S I$, and $-k_S M$ to the corresponding equations for C, I, and M in Eq. (2). Adding similar terms to Eq. (3) accounts for splitting there also.

Since these terms can be absorbed into preexisting terms, usually by augmenting the appropriate death rates by k_S, the foregoing analyses can be adapted to the possibility of splitting the cultures. In general, as

long as healthy cell reproduction can maintain constant cell concentrations against splitting, which is typical under actual conditions, the augmented death rates slow the short-time exponential growth of infection and enhance damping in the medium-time oscillations in infection.

4. PARAMETER VALUES

Default in vitro parameter values and typical ranges are given in Table 1. (Of course, in vitro parameter values often differ from corresponding in vivo values [6].) All parameter values are based on T cell lines, e.g., CEM cells, and will vary, depending on the particular experimental system and culture conditions used. Some of the values were determined as follows.

If dead cells and cellular debris diminish the vitality of the culture only slightly ($\gamma \approx 0$), their reproductive influences are felt only at extremely long times. Thus we arbitrarily set $\gamma = 0$. Similarly, in the absence of data, the relative efficiency of viral attachment to dead vs live cells was set by default to $\epsilon = 0$.

For Eq. (2) tissue culture experiments determined the typical parameter range for the infection rate constant k_I as follows. Assume for the moment that viral transmission occurs purely through cell-to-cell spread. The second theory referred to in the Introduction determined an empirical exponential growth rate k_e characterizing the initial growth of HIV-1 in tissue cultures [15]. Since Section 4.1.1 gives an initial exponential growth rate of $k_e = k_I C - \mu_I$, where C is the initial concentration of healthy cells, typically around 5×10^5 cells/ml, the parameter values in Table 1 imply that k_I is about 2×10^{-6} ml/day.

For Eq. (3), the same tissue culture experiments were used to determine the proportion σ of HIV-1 virions that successfully infect their cell after attaching, but in this case cell-free virions, not cell-to-cell contacts, were assumed to be the dominant mode of viral transmission. Section 3.2.2 then gives the empirical rate k_e as $k_e = r_S c^* - \mu_I = r_P \sigma - \mu_I$, since the initial reduced concentration c^* of healthy cells in the experiment was about 1. The measured empirical constant k_e of between 0.3 to 1.5 day^{-1} now yields a σ of about 5×10^{-4}, in interesting agreement with the ratio of defective to infectious virions, usually given as more than 1000 to 1 [15, 26].

5. NUMERICAL SOLUTIONS

This section gives numerical results from Eqs. (2) and (3) to illustrate some features of the models. Figures 1 and 2 and 3 show numerical solutions of Eq. (2) and (3) with parameter values in Table 1, unless otherwise specified.

In Fig. 1A for cell-to-cell spread, there is an initial phase of approximately exponential viral growth. The infection then reaches a peak, followed by a second phase characterized by damped, or overdamped, oscillation of the viral load. Such infective oscillations are to be expected from Eq. (2), which is essentially a Lotka–Volterra predator–prey model [18, p. 71; 19].

Figure 1B demonstrates the effect of splitting the culture continuously to match the cellular growth rate. The infective oscillations seen in Fig. 1A have disappeared, as predicted in Section 3.3.

Figure 2 for spread by cell-free virions resembles the corresponding Fig. 1. Other simulations (not shown) demonstrate the quasi-steady state given by Eq. (7) with an approximate proportionality of cell-free virions and infected cells. They also confirm the establishment of the quasi-steady state within a single generation of infected cells, if the total cell concentration remains relatively constant.

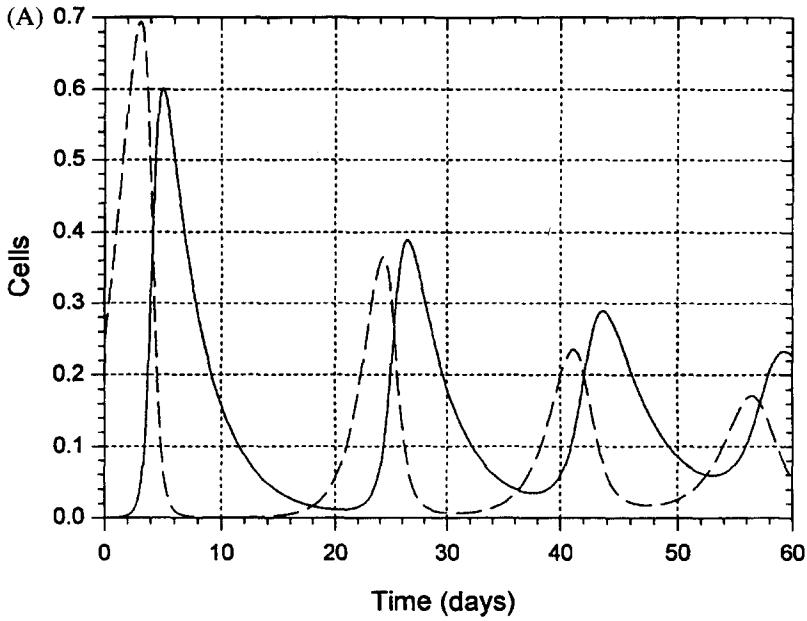

FIG. 1. Numerical simulation of HIV-1 infection kinetics in tissue culture: Eq. (2) for cell-to-cell transmission of the virus—the effect of splitting the tissue cultures. For convenience, the Y-axis uses dimensionless variables: dimensionless healthy cell concentration $C^* = C/C_m$ (dashed line) and dimensionless infected cell concentration $I^* = I/C_m$ (solid line). Table 1 gives the appropriate default and initial values, with $C^*(0) = 0.25$ and $I^*(0) = 0.00025$, except that (A) there was no splitting, i.e., $k_S = 0$, and (B) the culture was split to match the cellular reproductive rate, $k_S = \tau$.

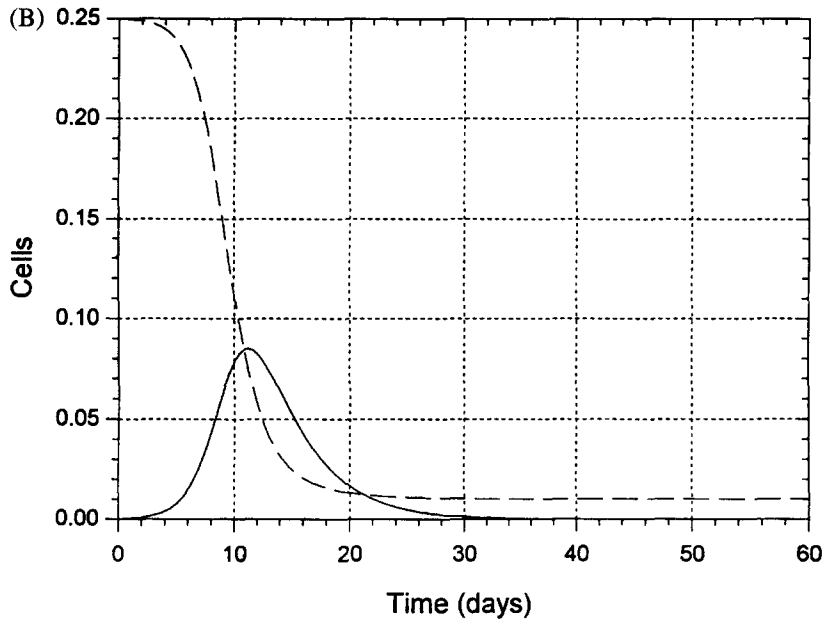

FIG. 1. (*Continued*).

As in Fig. 1B, Fig. 2B demonstrates the effect of splitting the culture continuously to match the cellular growth rate. The infective oscillations seen in Fig. 2A have disappeared, as predicted in Section 3.3.

The maximum concentration of virions in Figs. 2A and 2B is about 10^8 ml^{-1}. While it is more than the concentration of viral RNA seen in vivo, around 10^5–10^6 ml^{-1} [27, 28], it is also consistent with experiments showing a 10^9–10^{10} ml^{-1} concentration of physical particles in stocks with maximized infectivity [26].

Figs. 3, for spread by cell-free virions like Figs. 2, demonstrate that infective oscillations are damped by the attachment of cell-free virus to dead cells and cellular debris. In both Figs. 2A and 3A, virus does not attach to dead cells ($\epsilon = 0$). An extra curve in Fig. 3A displays the accumulation of dead cells and cellular debris. Fig. 3B shows that the infective oscillations are completely damped when virus attaches equally well to live and dead cells ($\epsilon = 1$). When viral cultures are split, simulations (not shown) demonstrated similar damping effects.

Section 3.1.1 indicates that changing cell concentrations changes the rate of cell-to-cell viral spread. On the other hand, Eq. (9) predicts that under cell-free viral spread, the initial exponential rate of viral growth k_e is indifferent to absolute cell concentrations, as long as the quasi-steady-state relation Eq. (7) holds. Numerical simulations showed that

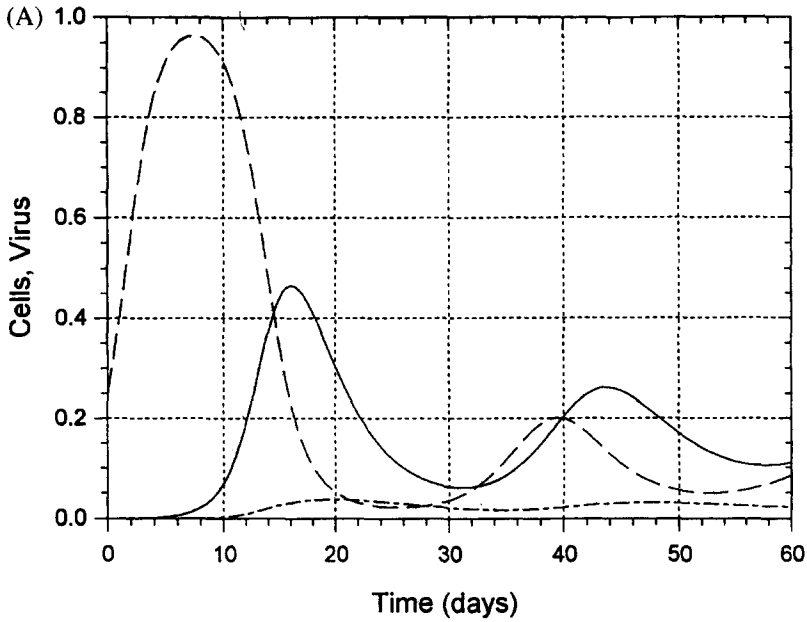

FIG. 2. Numerical simulation of HIV-1 infection kinetics in tissue culture: Eq. (2) for transmission by cell-free virus—the effect of splitting cultures. For convenience, the Y-axis uses dimensionless variables: dimensionless healthy cell concentration $C^* = C/C_m$ (dashed line), dimensionless infected call concentration $I^* = I/C_m$ (solid line), and dimensionless viral concentration $V^* = V/V_m$ (short dashed-dotted line), where $V_m = 2\times10^9$ ml^{-1} provides a convenient scale. Table 1 gives the appropriate default and initial values, with $C^*(0) = 0.25$, $I^*(0) = 0$, and $V^*(0) = 0.00025$, (A) except that there was no splitting $k_S = 0$, and (B) the culture was split to match the cellular reproductive rate: $k_S = r$.

requirement for a quasi-steady state, particularly at the culture's initiation, was stringent. Taking a chronically infected culture whose total cell concentration is the same as the target culture, mixing it thoroughly, and then pipetting cells and supernatant together from it into the target culture might conceivably satisfy this requirement. The value of conclusions about cell-to-cell vs cell-free viral spread based on these kinetic predictions is of dubious value, however, because they appear so sensitive to the experimental conditions.

6. DISCUSSION

This article has developed models of HIV-1 infection kinetics in tissue cultures that quantitatively describe the two different modes of viral spread, cell-to-cell contact and infection through cell-free virus. Although our approach, which is based on phenomenological descrip-

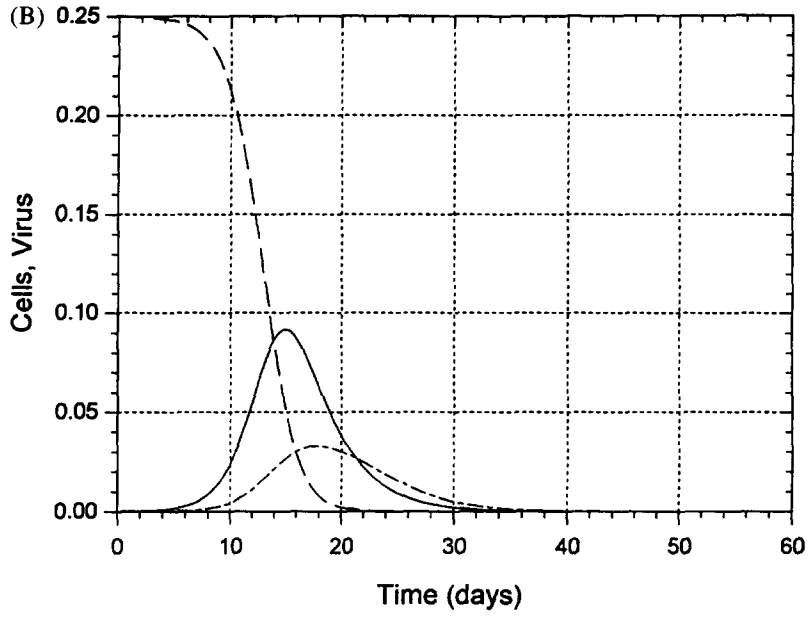

FIG. 2. (*Continued*).

tion of virus-cell interactions, is able to mimic experimental patterns of virus spread, more experimental work under strictly defined conditions is needed to resolve several important issues.

Under certain conditions, cell-to-cell spread may be more effective than cell-free spread in transmitting virus [15–17]. These conditions have not been precisely defined but may be extremely important. An infectious HIV-1 virion typically has about one attachment opportunity during a 1-h incubation in 5×10^5 cells/ml [9]. For a viral strain taking on the order of 10 h for spontaneous inactivation (a typical figure for some, but not all HIV-1 strains [13]), as long as the cell concentration remains above about 5×10^4 cells/ml, an infectious virion in suspension usually attaches to a cell before inactivating. Since attachment occupies a relatively brief time in the HIV-1 replication cycle, variations in cell concentrations should therefore have little impact on cell-free spread. On the other hand, if cell-to-cell spread predominates, any increase in cell concentration should increase the frequency of cell-to-cell contacts, and consequently the infection rate (as long as the system is well mixed, so transmission is seldom restricted to cell aggregates). Thus a series of experiments in which cell concentrations are systematically varied could theoretically address which of the two modes of transmission predominates, but numerical simulations indicated great practical difficulties in

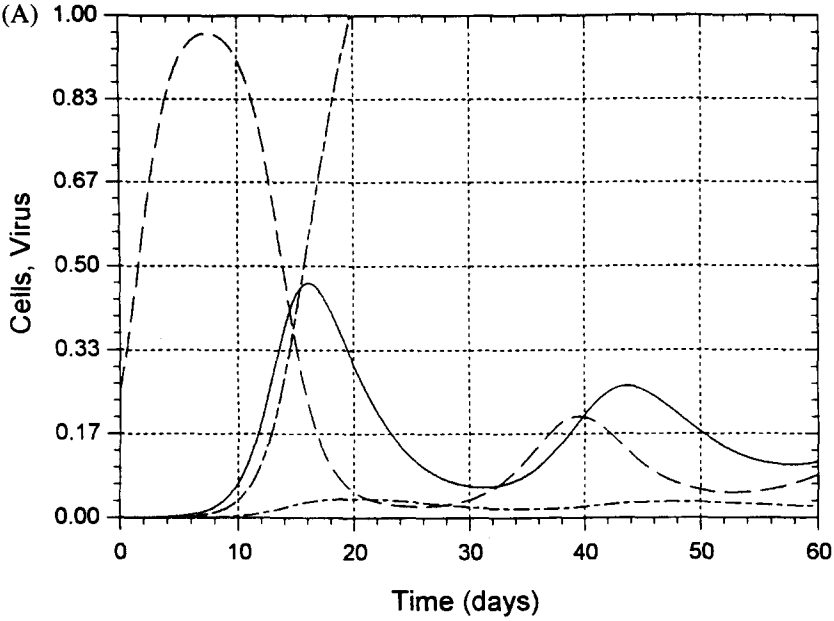

FIG. 3. Numerical simulation of HIV-1 infection kinetics in tissue culture: Eq. (2) for transmission by cell-free virus—with damping ($\epsilon = 1$). For convenience, the Y-axis uses dimensionless variables: dimensionless healthy cell concentration $C^* = C/C_m$ (dashed line), dimensionless infected cell concentration $I^* = I/C_m$ (solid line), dimensionless concentration of cells that have died $M^* = M/C_m$ (long dashed-dotted line), and dimensionless viral concentration $V^* = V/V_m$ (short dashed-dotted line), where $V_m = 2 \times 10^9$ ml^{-1} provides a convenient scale. Table 1 gives the appropriate default and initial values, with $C^*(0) = 0.25$, $I^*(0) = 0$, $M^*(0) = 0$, and $V^*(0) = 0.00025$. (A) Virions do not attach to dead cells and cellular debris ($\epsilon = 0$), and (B) virions attach to dead cells and cellular debris as fast as they attach to live cells ($\epsilon = 1$).

interpreting the corresponding experiments for reasons given at the end of Section 5. The negative results from the simulations indicate that experiments distinguishing between cell-to-cell and cell-free viral spread must make the distinction on qualitative, not quantitative, grounds. Thus experiments disturbing cell-to-cell contacts through shaking, pipetting, or otherwise may be required to distinguish cell-to-cell spread from cell-free spread in cultures.

The preceding arguments, if applied in vivo, indicate that cell-to-cell spread should be particularly efficient in lymph nodes, where cell concentration is 10^8 cells/ml. If cell-to-cell spread does indeed dominate infection kinetics in vivo, confirming that cell-to-cell spread pre-

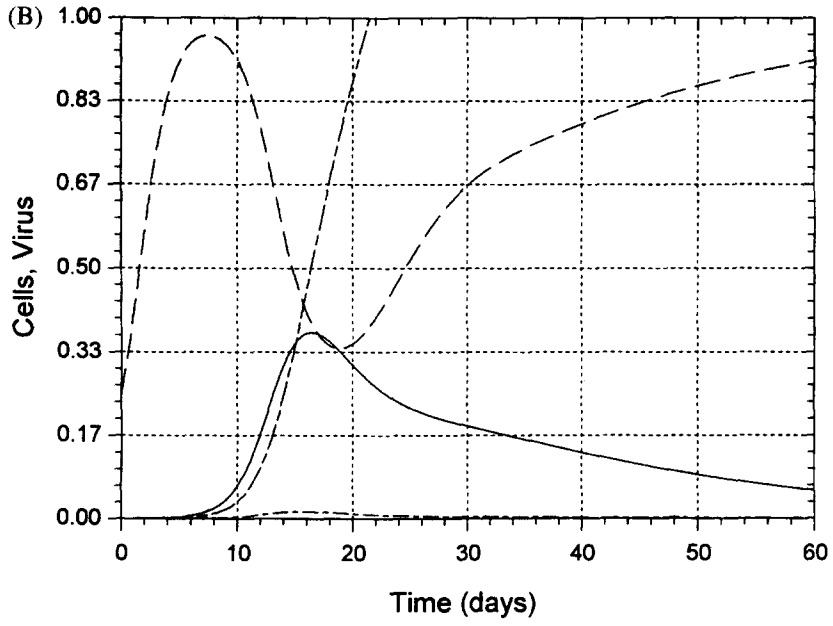

FIG. 3. (*Continued*).

dominates in vitro therefore seems a desirable preamble to using a model culture system to test antiviral efficacy.

Cellular aggregation and its effect on cell-to-cell spread in any particular culture system need to be addressed on a case-by-case basis, since viral transmission is probably very efficient within the aggregates, but it may be poor between them. Although splitting and diluting cultures can disrupt cellular aggregates and promote cell-to-cell contacts, the cells may aggregate later, and aggregation is particularly prominent at low cell concentrations, even down to 100 cells/ml. In contrast, however, suspension virions usually mix well with cells in many (but not all) systems [21–25].

Numerical simulations confirmed that in realistic parameter regimes, if the total cell concentration is kept relatively constant, the concentrations of infected cells and cell-free virus are nearly proportional to one another within the first generation of infected cells (the quasi-steady-state approximation in Section 3.2.1) [6]. All else equal, many different measures of infection (e.g., in situ PCR, immunostaining, or syncitial formation of infected calls, or p24 or reverse transcriptase assays of the supernatant) should therefore also be approximately proportional. Thus our simulations are consistent with implicit experimental presumptions

about the approximate equivalence of different measures of the viral load, although this equivalence may depend on holding the total cell concentration relatively constant.

The simulations also showed (see Figs. 1 and 2) that in a typical tissue culture infection starting with a small fraction of cells infected, the models of both cell-free viral spread and direct cell-to-cell transmission give an initial phase of exponential viral growth. With cell-free viral spread, if the infection does not peter out, the infection then reaches a peak, followed by a second phase characterized by mixed exponential growth and oscillation of the viral load, the parameters determining the relative importance (if any) of the exponential growth and oscillation. The second phase of cell-to-cell spread is similar, except that the viral load has a purely oscillatory character. With each type of spread, the initial oscillation in the second phase may be violent enough to extinguish the culture. If not, in each case the oscillation continues, damped or undamped, until eventually a third phase characterized by a gradual buildup of dead cells and cellular debris extinguishes the culture.

Oscillatory behavior is common in the predator–prey relationship postulated by our models between infected cells (or virus) and healthy cells: In classic predator–prey models, the predator population follows the oscillations in the prey population, but with a time lag [18, 19]. We had not expected, however, that our models would produce infective oscillations in typical tissue culture parameter regimes. Previously, models of in vivo HIV-1 infection were known to oscillate, but only in parameter regimes unrealistic in vivo [6]. We were even more surprised, however, to discover that experimental tissue cultures could display several sequential cycles of oscillation (G. Englund, personal communication), and that the corresponding data permitted our models to give a quantitative fit within realistic parameter ranges (Dimitrov et al., manuscript in preparation).

Our models indicate that infective oscillation is damped by attachment of cell-free virus to dead cells and cellular debris, which effectively decoys transmission by cell-free virus (see Fig. 3). Dilution during splitting similarly damps infective oscillation. Since many long-term cultures are split, this may explain why sequential cycles of oscillation are rarely observed in cultures.

Infective oscillations are sometimes observed in tissue culture experiments, and although predator–prey models provide a natural explanation, oscillations can have other causes. Defective virions, for example, may cause them by the mechanism of interference, as follows. HIV-1 has a high ratio of defective to infecting virions (more than 1000 to 1 [15, 26]). When a large concentration of defective virions or viral products (e.g., free gp120) is present, binding to receptor molecules

(e.g., CD4) on uninfected cells can interfere with infection and protect healthy cells. The infected cells then will decrease along with the viral load, reducing interference, leaving the healthy cells unprotected, and opening them to infection once again. The viral load then increases and the cycle repeats. When most of the cells are infected, the interference could be significant, but even then only under the most extreme conditions: The concentration of gp120 would have to be about 1 μg/ml to protect CD4+ cells from infection. Although an observed infective oscillation may also be caused by cellular subpopulations, viral strains with differing infectivities (so-called "revertants"), etc., we have shown in this article that the oscillations can be explained by the dynamics of viral transmission alone. The dynamic explanation would find support if using the putative revertant instead of the original viral inoculum under duplicate culture conditions reproduces the original oscillation. Significantly, however, two very natural models of viral infection both give oscillations in realistic parameter regimes. If any other potentially more interesting, more biological explanation has important implications, it also requires independent experimental support.

Finally, in vitro experiments are often extrapolated to in vivo situations, but many factors can alter in vivo patterns of HIV-1 infection. For example, several groups recently reported on changes in the viral load and CD4+ cell concentration after administering potent HIV-1 inhibitors to AIDS patients [27, 28]. Interestingly, one calculation indicated a half-life of about 2 days for cells acutely infected with HIV-1, a figure extremely close to the half-life found in vitro for acutely infected cells [29]. Since this calculation made several assumptions of unknown validity about the trafficking of cells between different compartments, and since the rules governing immune trafficking and regulation in vivo are not well understood [30–33], however, we end on a cautionary note: Conclusions drawn from tissue culture infections need to be examined very carefully before applying them to more complex in vivo systems.

REFERENCES

1 M. Debrueck, The growth of bacteriophage and lysis of the host. *J. Gen. Physiol.* 23:631–642 (1940).

2 M. Delbrueck, The growth of of bacteriophage and lysis of the host. *J. Gen. Physiol.* 23:643–660 (1940).

3 R. Dulbecco, Production of plaques in monolayer tissue cultures by single particles of an animal virus. *Proc. Natl. Acad. Sci. USA* 38:747–752 (1952).

4 R. Dulbecco, M. Vogt, and A. G. R. Strickland, A study of the basic aspects of neutralization of two animal viruses, western equine encephalitis virus and poliomyelitis virus. *Virology* 2:162–205 (1956).

5 E. L. Ellis and M. Delbrueck, The growth of bacteriophage. *J. Gen. Physiol.* 22:365–384 (1939).

6 A. S. Perelson, D. E. Kirschner, and R. de Boer, Dynamics of HIV infection of CD4+ T cells. *Math. Biosci.* 114:81–125 (1992).

7 J. J. Bailey, J. E. Fletcher, E. T. Chuck, and R. I. Shrager, A kinetic model of CD4+ lymphocytes with the human immunodeficiency virus HIV. *Biosystems* 26:177–183 (1992).

8 S. P. Layne, J. L. Spouge, and M. Dembo, Quantifying the infectivity of human immunodeficiency virus. *Proc. Natl. Acad. Sci. USA* 86:4644–4648 (1989).

9 J. L. Spouge, Viral multiplicity of attachment and its implications for HIV therapies. *J. Virol.* 68:1782–1789 (1994).

10 S.-C. Wu, J. L. Spouge, S. L. Conley, W.-P. Tsai, and P. L. Nara, Human plasma enhances the infectivity of primary human immunodeficiency virus type 1 isolates in peripheral blood mononuclear cells and monocyte-derived macrophages. *J. Virol.* 69:6054–6062 (1995).

11 S. L. Orloff, M. S. Kennedy, A. A. Belperron, P. J. Maddon, and J. S. McDougal, Two mechanisms of soluble CD4 (sCD4)-mediated inhibition of human immunodeficiency virus type 1 (HIV-1) infectivity and their relation to primary HIV-1 isolates with reduced sensitivity to sCD4. *J. Virol.* 67:1461–1471 (1993).

12 S. P. Layne, M. J. Merges, M. Dembo, J. L. Spouge, and P. L. Nara, HIV requires multiple gp120 molecules for CD4-mediated infection. *Nature (London)* 346:277–279 (1990).

13 S. P. Layne, M. J. Merges, J. L. Spouge, M. Dembo, and P. L. Nara, Blocking of human immunodeficiency virus infection depends on cell density and viral stock age. *J. Virol.* 65:3293–3300 (1991).

14 D. S. Dimitrov, R. L. Willey, M. A. Martin, and R. Blumenthal, Kinetics of HIV-1 interactions with sCD4 and CD4+ cells: Implications for inhibition of virus infection and initial steps of virus entry into cells. *Virology* 187:398–406 (1992).

15 D. S. Dimitrov, R. L. Willey, H. Sato, L.-J. Chang, R. Blumenthal, and M. A. Martin, Quantitation of human immunodeficiency virus type 1 infection kinetics. *J. Virol.* 67:2182–2190 (1993).

16 H. Sato, J. Orenstein, D. S. Dimitrov, and M. A. Martin, Cell-to-cell spread of HIV-1 occurs within minutes and may not involve the participation of virus particles. *Virology* 186:712–724 (1992).

17 D. M. Philips, The role of cell-to-cell transmission in HIV infection. *AIDS* 8:719–731 (1994).

18 J. D. Murray, *Mathematical Biology*, New York, Springer-Verlag, 1989.

19 F. M. Scudo and J. R. Ziegler, *The Golden Age of Theoretical Ecology: 1923–1940*, New York, Springer-Verlag, 1978.

20 S. Kim, R. Byrn, J. Groopman, and D. Baltimore, Temporal aspects of DNA and RNA synthesis during human immunodeficiency virus infection: Evidence for differential gene expression. *J. Virol.* 63:3708–3713 (1989).

21 L. Philipson, *The Early Interaction of Animal Viruses and Cells*, Vol. 5, Karger, New York, 1963, pp. 43–78.

22 R. C. Valentine and A. C. Allison, Virus particle adsorption. I. Theory of adsorption and experiments on the attachment of particles to non-biological surfaces. *Biochim. Biophys. Acta* 34:10–23 (1959).

23 A. C. Allison and R. C. Valentine, Virus particle adsorption. II. Adsorption of vaccinia and fowl plague viruses to cells in suspension. *Biochim. Biophys. Acta* 40:393–399 (1960).

24 A. C. Allison and R. C. Valentine, Virus particle adsorption. III. Adsorption of viruses by cell monolayers and effects of some variables on adsorption. *Biochim. Biophys. Acta* 40:400–410 (1960).

25 R. A. Chillakuru, D. D. Y. Ryu, and T. Yilma, Propagation of recombinant vaccinia virus in hela cells: Adsorption kinetics and replication in batch cultures. *Biotechnol. Prog.* 7:85–92 (1991).

26 S. P. Layne, M. J. Merges, M. Dembo, J. L. Spouge, S. R. Conley, J. P. Moore, J. L. Raina, J. H. Renz, H. R. Gelderblom, and P. L. Nara, Factors underlying spontaneous inactivation and susceptibility to neutralization of Human Immunodeficiency Virus. *Virology* 189:3293–3300 (1992).

27 D. D. Ho, A. U. Neumann, A. S. Perelson, W. Chen, J. M. Leonard, and M. Markowitz, Rapid turnover of plasma virions and CD4 lymphocytes in HIV-1 infection. *Nature* 373:123–126 (1995).

28 X. Wei, S. K. Ghosh, M. E. Taylor, V. A. Johnson, E. A. Emini, P. Deutsch, J. D. Lifson, S. Bonhoeffer, M. A. Nowak, B. H. Hahn, M. S. Saag, and G. M. Shaw, Viral dynamics in human immunodeficiency virus type 1 infection. *Nature* 373:117–122 (1995).

29 R. Leonard, D. Zagury, I. Desportes, J. Bernard, J.-F. Zagury, and R. C. Gallo, Cytopathic effect of human immunodeficiency virus in T4 cells is linked to the last stage of virus infection. *roc. Natl. Acad. Sci. USA* 85:3570–3574 (1988).

30 D. E. Mosier, HIV results in the frame: CD4+ cell turnover. *Nature* 375:193–194 (1995).

31 J. Sprent and D. Tough, HIV results in the frame: CD4+ cell turnover. *Nature* 375:194 (1995).

32 M. S. Ascher, H. W. Sheppard, R. W. Anderson, J. F. Krowka, and H. J. Bremermann, HIV results in the frame: Paradox remains. *Nature* 375:196 (1995).

33 D. S. Dimitrov and M. A. Martin, HIV results in the frame: CD4+ cell turnover. *Nature* 375:194–195 (1995).